

Discovery of cancer driver genes based on nucleotide context

1
2
3
4

Felix Dietlein^{1,2,6*}, Donate Weghorn^{3,4,6}, Amaro Taylor-Weiner^{1,2}, André Richters^{2,5}, Brendan Reardon^{1,2}, David Liu^{1,2}, Eric S. Lander², Eliezer M. Van Allen^{1,2,7*} & Shamil R. Sunyaev^{3,4,7*}

5

6 **Many cancer genomes contain large numbers of somatic mutations, but few of these**
7 **mutations drive tumor development. Current approaches to identify cancer driver genes**
8 **are largely based on mutational recurrence, i.e. they search for genes with an increased**
9 **number of nonsynonymous mutations relative to the local background mutation rate.**
10 **Multiple studies have noted that the sensitivity of recurrence-based methods is limited in**
11 **tumors with high background mutation rates, because passenger mutations dilute their**
12 **statistical power. Here, we observe that passenger mutations tend to occur in characteristic**
13 **nucleotide sequence contexts, while driver mutations follow a different distribution**
14 **pattern determined by the location of functionally relevant genomic positions along the**
15 **protein-coding sequence. To discover new cancer genes, we searched for genes with an**
16 **excess of mutations in unusual nucleotide contexts that deviate from the characteristic**
17 **context around passenger mutations. By applying this statistical framework to whole-**
18 **exome sequencing data from 12,004 tumors, we discovered a long tail of novel candidate**
19 **cancer genes with mutation frequencies as low as 1% and functional supporting evidence.**
20 **Our results show that considering both the number and the nucleotide context around**
21 **mutations helps identify novel cancer driver genes, particularly in tumors with high**
22 **background mutation rates.**

23

24 Multiple algorithms have been developed to systematically identify genes that drive tumor
25 formation¹⁻⁵. Most search for genes harboring more nonsynonymous mutations than expected
26 based on the local background mutation rate¹⁻⁵. These recurrence-based methods have
27 successfully identified many novel cancer genes^{4,6,7}. However, several studies have noted that the
28 sensitivity of recurrence-based approaches is limited^{6,8,9}, because functionally neutral passenger
29 mutations dilute their statistical power to detect recurrent driver mutations^{10,11}. Hence, due to the
30 high prevalence of passenger mutations in tumors with high background mutation rates, recent
31 studies have concluded that orders of magnitude more sequencing data would be needed to
32 establish a comprehensive catalog of all cancer driver genes using recurrence-based methods^{6,8,9}
33 (Fig. S1).

34 Passenger mutations are not uniformly distributed along the cancer genome. Rather, they are
35 enriched within characteristic nucleotide sequence contexts, whose specificity depends on the
36 specific mutational processes active in a given tumor¹²⁻¹⁵. For instance, APOBEC enzymes scan
37 single-stranded DNA for specific nucleotide sequence motifs and deaminate cytidine to uracile
38 within these motifs¹⁶⁻¹⁸. Similarly, mutant polymerase ϵ randomly introduces passenger mutations
39 in a non-uniform manner, since its fidelity depends strongly on the local nucleotide context¹⁹⁻²².
40 For driver mutations, the distribution depends not only on the local nucleotide context, but also on
41 the location of functionally relevant positions along the protein sequence²³⁻²⁶. Thus, we
42 hypothesized that the nucleotide context would differ substantially around driver and passenger
43 mutations.

44 Based on this hypothesis, we here developed a biologically informed statistical approach for
45 discovering new cancer genes. Briefly, our approach searches for genes harboring an excess of
46 mutations in unusual nucleotide contexts that deviate from the characteristic nucleotide context
47 around passenger mutations (Fig. 1a, Methods).

48 Our new method requires modeling the nucleotide context around passenger mutations. The 5'
49 and 3' nucleotides immediately adjacent to a passenger mutation have the strongest effect on the
50 local mutation probability (Fig. 1b, S2-S3). However, as reported previously^{27,28}, the additional
51 upstream and downstream nucleotides flanking a passenger mutation also influence its mutation
52 probability substantially (Fig. 1b, S2-S3). Traditionally, the effect of the flanking 5' and 3'
53 nucleotides on the local mutation probability has been modeled by determining the mutation
54 probabilities of all possible trinucleotide contexts independently¹²⁻¹⁵. As the number of flanking

55 nucleotides increases, the number of possible sequence contexts grows exponentially - soon
56 exceeding the number of mutations per tumor (Fig. S4). Hence, it is no longer feasible to analyze
57 all possible sequence contexts independently.

58 Instead, we approximated the context-specific mutation probability by assuming that each
59 flanking nucleotide contributed independently and multiplicatively to the local mutation
60 probability (Fig. 1c-f, S5-S8, Methods). For instance, we approximated the mutation probabilities
61 of trinucleotide contexts as products of the effects of their flanking 5' and 3' nucleotides, as well as
62 their base substitution type (Fig. 1c-d, S7a). We developed a composite likelihood model²⁹ to
63 extend this approach to larger nucleotide contexts (Fig. 1e). This model closely matched the
64 observed mutation probabilities for the 29 cancer types examined in this study (Fig. 1e-f, S7b-c).
65 Although the immediately adjacent 5' and 3' nucleotides had the strongest impact on the local
66 mutation probability, also flanking nucleotides outside of the trinucleotide context had a
67 substantial effect in this composite likelihood model, thus refining our approximation of the local
68 mutation probabilities (Fig. S7d, S8).

69 We then examined whether the composite likelihood model could distinguish driver from
70 passenger mutations using 10 established melanoma genes and 5 non-cancer-related genes that
71 had been reported as false-positive findings in previous cancer gene discovery studies³ (Fig. 2).
72 While mutations in non-cancer-related genes closely followed the expected context-dependent
73 distribution pattern derived from the composite likelihood model, most mutations in cancer genes
74 fell in nucleotide contexts that deviated from the expectation of the model. This suggested that
75 considering the broad nucleotide context around mutations could indeed provide new biological
76 information to help distinguish between driver and passenger mutations.

77 Encouraged by these observations, we developed a statistical framework to detect cancer driver
78 genes that considers both mutation counts and nucleotide contexts. In our model, the probability
79 of observing the number n_g and the context-dependent distribution v_g of nonsynonymous
80 mutations in a gene g ($P(n_g, v_g | s_g; \lambda_g)$) depends on the number of synonymous mutations s_g and
81 the context-specific mutation rates λ_g . We decomposed this probability into the probability of
82 observing n_g nonsynonymous mutations, given the number of synonymous mutations
83 s_g ("mutation count"; $P(n_g | s_g)$), and the probability of these n_g nonsynonymous mutations falling

84 in nucleotide contexts v_g , given their context-specific mutation rates λ_g ("nucleotide context";
85 $P(v_g|n_g; \lambda_g)$):

86
$$P(n_g, v_g|s_g; \lambda_g) := \underbrace{P(n_g|s_g)}_{\text{mutation count}} \cdot \underbrace{P(v_g|n_g; \lambda_g)}_{\text{nucleotide context}} \quad (1)$$

87 Here, $P(n_g|s_g)$ reflects the established statistics used by existing recurrence-based methods for
88 cancer gene discovery¹⁻⁵. The *p*-value of $P(v_g|n_g; \lambda_g)$ was derived by comparing the observed
89 nucleotide contexts v_g against a large number of random scenarios generated by a Monte Carlo
90 simulation approach based on the same the context-specific mutation rates λ_g ^{30,31}. As shown by
91 Q-Q-plots³², the *p*-values derived from $P(n_g|s_g)$, $P(v_g|n_g; \lambda_g)$, and $P(v_g, n_g|s_g; \lambda_g)$ closely
92 approximated a uniform distribution, which indicated that our models were reasonably well
93 calibrated to the observed data (Fig. 3a, Methods).

94 Notably, mutational count and nucleotide context provided complementary criteria for detecting
95 cancer genes (Fig. 3a). In cancer types with low background mutation rates, such as thyroid
96 cancer, mutational counts were highly informative. In cancer types with high background
97 mutation rates, such as melanoma, the nucleotide context was the dominant criterion. Combining
98 both criteria identified several candidate cancer genes that could not be identified based on
99 mutational count or nucleotide context alone (Fig. 3a).

100 We applied our statistical framework to whole-exome sequencing data from 12,004 individual
101 tumors spanning 29 different tumor types (Fig. S9, Table S1). The results of these analyses are
102 summarized here (Fig. 3-4, S9-45) and at www.cancer-genes.org, for various false-discovery rate
103 (FDR) thresholds. For FDR<0.25, we identified 697 gene-tumor pairs, i.e. pairs of significantly
104 mutated genes and their associated tumor type. These gene-tumor pairs involved 379 distinct
105 genes, with 423 gene-tumor pairs being novel. The corresponding numbers were 484, 252 and
106 231 for FDR<0.05, as well as 395, 201, and 168 for FDR<0.01 (Tables 1, S2-S3). Gene-tumors pairs
107 were considered novel if they were not reported as significantly mutated in at least two
108 computational studies, among all TCGA marker papers, a meta-analysis of 876 publications, and
109 two large-scale pan-cancer gene discovery studies^{4,6,7,33}.

110 We next examined the biological relevance of the 423 novel gene- tumor pairs (FDR<0.25). Half of
111 the novel gene-tumor pairs (49%) involved canonical cancer genes in the Cancer Gene Census^{34,35},
112 compared with a rate of 3.8% for random gene-tumor pairs. We systematically reviewed the

113 literature to further investigate the experimental or clinical support for of the novel gene-tumor
114 pairs. We only considered publications with experimental data supporting the causal involvement
115 of these genes in carcinogenesis and excluded functionally unsupported reports of mutations
116 (Methods). A majority of the novel gene-tumor pairs (82%) had experimental support, with 61%
117 having support in the same tumor type, in which we detected them as significantly mutated (Fig.
118 3b, Tables 1, S2-S3). In contrast, the rate for random gene-tumor pairs was 17%. Overall, 11%
119 (75/697, FDR<0.25), 6% (30/484, FDR<0.05), and 4% (16/395, FDR<0.01) of the significant gene-
120 tumor pairs had no literature support, which is roughly in accordance with these FDR thresholds
121 (Fig. 3b, Tables 1, S2-S3).

122 We asked whether considering the nucleotide context identified candidate cancer genes that were
123 not discovered based on recurrence alone. Among gene-tumor pairs previously reported as
124 significantly mutated, 74% were also identified by using an established recurrence-based
125 approach³ (FDR<0.25 for both methods, Fig. 3c-d, S10). In contrast, among novel gene-tumor
126 pairs, only 33% were identified based on recurrence alone. In particular, our statistical framework
127 identified numerous biologically relevant candidate cancer genes that were not identified based
128 on recurrence alone. For instance, *HDAC4* (histone deacetylase 4) was significantly mutated in
129 gastroesophageal cancer (FDR=5.5x10⁻² by nucleotide context and recurrence; FDR=6.8x10⁻¹ by
130 recurrence alone; not reported as significant previously; Fig. 3e, S11). Histone deacetylases have
131 been implicated in tumor formation³⁶⁻³⁸ and *HDAC4* displayed two mutational hotspots: gastric
132 cancers with disruptive frameshift mutations (P901fs), and esophageal cancers with recurrent
133 missense mutations (F746L) (Fig. 3e). Similarly, we identified *POLR2A* (RNA polymerase II subunit
134 A) as significantly mutated in lung adenocarcinoma (FDR=1.07x10⁻⁵ by nucleotide context and
135 recurrence; FDR=1.0 by recurrence; not reported as significant previously; Fig. 4, S12). Mutations
136 in *POLR2A* have been implicated in the development of meningioma³⁹, and *POLR2A* has been
137 identified as a therapeutic target in colon cancer due to its frequent co-deletion with *TP53*⁴⁰.
138 Further, we noticed that *POLR2A* contained recurrent mutations in positions that are relevant for
139 the protein-DNA interaction (Fig. S12). Additional biologically relevant candidate cancer genes
140 that were not identified based on recurrence included *ANAPC1*, *FGFR4*, *IKZF3*, *PARG*, *SOX17*, and
141 *ZFX* (FDR<0.1 by nucleotide context and recurrence; FDR=1.0 by recurrence; Fig. 4, S11-S12,
142 Tables S2-S3). In addition, we observed that the following cancer-related signaling complexes
143 contained several candidate cancer genes, i.e. new cancer genes or gene-tumor pairs: modulation

144 of Ras signaling (*RHOA*, *RHOB*, *RRAS2*), cell cycle regulation (*CCNQ*, *CDK4*), regulation of protein
145 levels (*EEF1A1*, *EIF1AX*, *MIA2*), the catenin/cadherin complex (*FAT1*, *FAT3*, *FAT4*), DNA
146 polymerases (*POLQ*, *POLR2A*, *REV3L*), regulation of transcription (*MAML2*, *SF3B2*), modulation of
147 apoptosis (*ACVR2A*, *ACVR1B*, *CASP8*, *BIRC3*, *BIRC6*), and epigenetic modification (Fig. S13). In these
148 signaling complexes, 64% (118/183) of the gene-tumor pairs had not been reported as
149 significantly mutated previously, and 60% (110/183) of the gene-tumor pairs were not identified
150 by recurrence alone (Fig. 4).

151 Taken together, our findings demonstrate that characterization of the broad nucleotide context
152 around somatic passenger mutations enhances cancer gene discovery, particularly in tumor types
153 with high background mutation rates. Consideration of the nucleotide context for cancer gene
154 discovery does not require prior knowledge of the location of functionally relevant positions or
155 the biological effect of mutations. Hence, nucleotide contexts may ultimately be amenable to
156 variant and gene discovery in non-coding regions of the cancer genome. Through our statistical
157 model we identified a long tail of reasonable candidate cancer genes that may form the foundation
158 for future experimental and clinical studies. The new statistical framework is available as a fully
159 executable software tool called MutPanning (www.cancer-genes.org) and can be executed online
160 as a module on the GenePattern platform⁴¹ (www.genepattern.org).

161

162 **Acknowledgments**

163 We thank Dr. Gad Getz for valuable comments and suggestions. F.D. was supported by EMBO
164 (ALTF 502-2016). E.M.V.A. and S.R.S received funding from the National Institutes of Health (K08
165 CA188615, R01 CA227388 to E.M.V.A; R01 MH101244, R35 GM127131, U01 HG009088 to S.R.S.).
166 E.M.V.A further acknowledges support by the Phillip A. Sharp Innovation in Collaboration Award.

167

168 **Competing interests**

169 E.M.V. is a consultant for Tango Therapeutics, Genome Medical, Invitae, Foresite Capital, Dynamo,
170 and Illumina. E.M.V. received research support from Novartis and BMS, as well as travel support
171 from Roche and Genentech. E.M.V. is an equity holder of Syapse, Tango Therapeutics, Genome
172 Medical.

173

174

175 **References**

- 176 1. Dees, N.D. *et al.* MuSiC: identifying mutational significance in cancer genomes. *Genome Res*
177 **22**, 1589-98 (2012).
- 178 2. Gonzalez-Perez, A. & Lopez-Bigas, N. Functional impact bias reveals cancer drivers. *Nucleic*
179 *Acids Res* **40**, e169 (2012).
- 180 3. Lawrence, M.S. *et al.* Mutational heterogeneity in cancer and the search for new cancer-
181 associated genes. *Nature* **499**, 214-218 (2013).
- 182 4. Martincorena, I. *et al.* Universal Patterns of Selection in Cancer and Somatic Tissues. *Cell*
183 **171**, 1029-1041 e21 (2017).
- 184 5. Weghorn, D. & Sunyaev, S. Bayesian inference of negative and positive selection in human
185 cancers. *Nat Genet* **49**, 1785-1788 (2017).
- 186 6. Lawrence, M.S. *et al.* Discovery and saturation analysis of cancer genes across 21 tumour
187 types. *Nature* **505**, 495-501 (2014).
- 188 7. Hoadley, K.A. *et al.* Cell-of-Origin Patterns Dominate the Molecular Classification of 10,000
189 Tumors from 33 Types of Cancer. *Cell* **173**, 291-304 e6 (2018).
- 190 8. Hofree, M. *et al.* Challenges in identifying cancer genes by analysis of exome sequencing
191 data. *Nat Commun* **7**, 12096 (2016).
- 192 9. Tokheim, C.J., Papadopoulos, N., Kinzler, K.W., Vogelstein, B. & Karchin, R. Evaluating the
193 evaluation of cancer driver genes. *Proc Natl Acad Sci U S A* **113**, 14330-14335 (2016).
- 194 10. Guo, M.H. *et al.* Determinants of Power in Gene-Based Burden Testing for Monogenic
195 Disorders. *Am J Hum Genet* **99**, 527-539 (2016).
- 196 11. Lee, S., Abecasis, G.R., Boehnke, M. & Lin, X. Rare-variant association analysis: study designs
197 and statistical tests. *Am J Hum Genet* **95**, 5-23 (2014).
- 198 12. Alexandrov, L.B. *et al.* Signatures of mutational processes in human cancer. *Nature* **500**,
199 415-21 (2013).
- 200 13. Alexandrov, L.B. *et al.* Mutational signatures associated with tobacco smoking in human
201 cancer. *Science* **354**, 618-622 (2016).
- 202 14. Nik-Zainal, S. *et al.* Mutational processes molding the genomes of 21 breast cancers. *Cell*
203 **149**, 979-93 (2012).
- 204 15. Nik-Zainal, S. *et al.* Landscape of somatic mutations in 560 breast cancer whole-genome
205 sequences. *Nature* **534**, 47-54 (2016).
- 206 16. Ebrahimi, D., Alinejad-Rokny, H. & Davenport, M.P. Insights into the motif preference of
207 APOBEC3 enzymes. *PLoS One* **9**, e87679 (2014).
- 208 17. Roberts, S.A. *et al.* Clustered mutations in yeast and in human cancers can arise from
209 damaged long single-strand DNA regions. *Mol Cell* **46**, 424-35 (2012).
- 210 18. Roberts, S.A. *et al.* An APOBEC cytidine deaminase mutagenesis pattern is widespread in
211 human cancers. *Nat Genet* **45**, 970-6 (2013).
- 212 19. Church, D.N. *et al.* DNA polymerase epsilon and delta exonuclease domain mutations in
213 endometrial cancer. *Hum Mol Genet* **22**, 2820-8 (2013).
- 214 20. Shinbrot, E. *et al.* Exonuclease mutations in DNA polymerase epsilon reveal replication
215 strand specific mutation patterns and human origins of replication. *Genome Res* **24**, 1740-
216 50 (2014).
- 217 21. Goodman, M.F. & Fygenson, K.D. DNA polymerase fidelity: from genetics toward a
218 biochemical understanding. *Genetics* **148**, 1475-82 (1998).

219 22. Ganai, R.A. & Johansson, E. DNA Replication-A Matter of Fidelity. *Mol Cell* **62**, 745-55
220 (2016).

221 23. Chakravorty, D. *et al.* MYCbase: a database of functional sites and biochemical properties of
222 Myc in both normal and cancer cells. *BMC Bioinformatics* **18**, 224 (2017).

223 24. Izarzugaza, J.M., Redfern, O.C., Orengo, C.A. & Valencia, A. Cancer-associated mutations are
224 preferentially distributed in protein kinase functional sites. *Proteins* **77**, 892-903 (2009).

225 25. Chang, M.T. *et al.* Identifying recurrent mutations in cancer reveals widespread lineage
226 diversity and mutational specificity. *Nat Biotechnol* **34**, 155-63 (2016).

227 26. Chang, M.T. *et al.* Accelerating Discovery of Functional Mutant Alleles in Cancer. *Cancer*
228 *Discov* **8**, 174-183 (2018).

229 27. Shiraishi, Y., Tremmel, G., Miyano, S. & Stephens, M. A Simple Model-Based Approach to
230 Inferring and Visualizing Cancer Mutation Signatures. *PLoS Genet* **11**, e1005657 (2015).

231 28. Fredriksson, N.J. *et al.* Recurrent promoter mutations in melanoma are defined by an
232 extended context-specific mutational signature. *PLoS Genet* **13**, e1006773 (2017).

233 29. Varin, C., Reid, N. & Firth, D. AN OVERVIEW OF COMPOSITE LIKELIHOOD METHODS.
234 *Statistica Sinica* **21**, 5-42 (2011).

235 30. North, B.V., Curtis, D. & Sham, P.C. A note on the calculation of empirical P values from
236 Monte Carlo procedures. *Am J Hum Genet* **71**, 439-41 (2002).

237 31. Ewens, W.J. On estimating P values by the Monte Carlo method. *Am J Hum Genet* **72**, 496-8
238 (2003).

239 32. Pearson, T.A. & Manolio, T.A. How to interpret a genome-wide association study. *JAMA* **299**,
240 1335-44 (2008).

241 33. Ainscough, B.J. *et al.* DoCM: a database of curated mutations in cancer. *Nat Methods* **13**,
242 806-7 (2016).

243 34. Forbes, S.A. *et al.* COSMIC: exploring the world's knowledge of somatic mutations in human
244 cancer. *Nucleic Acids Res* **43**, D805-11 (2015).

245 35. Futreal, P.A. *et al.* A census of human cancer genes. *Nat Rev Cancer* **4**, 177-83 (2004).

246 36. Glazkak, M.A. & Seto, E. Histone deacetylases and cancer. *Oncogene* **26**, 5420-32 (2007).

247 37. Li, Y. & Seto, E. HDACs and HDAC Inhibitors in Cancer Development and Therapy. *Cold*
248 *Spring Harb Perspect Med* **6**(2016).

249 38. Ropero, S. & Esteller, M. The role of histone deacetylases (HDACs) in human cancer. *Mol*
250 *Oncol* **1**, 19-25 (2007).

251 39. Clark, V.E. *et al.* Recurrent somatic mutations in POLR2A define a distinct subset of
252 meningiomas. *Nat Genet* **48**, 1253-9 (2016).

253 40. Liu, Y. *et al.* TP53 loss creates therapeutic vulnerability in colorectal cancer. *Nature* **520**,
254 697-701 (2015).

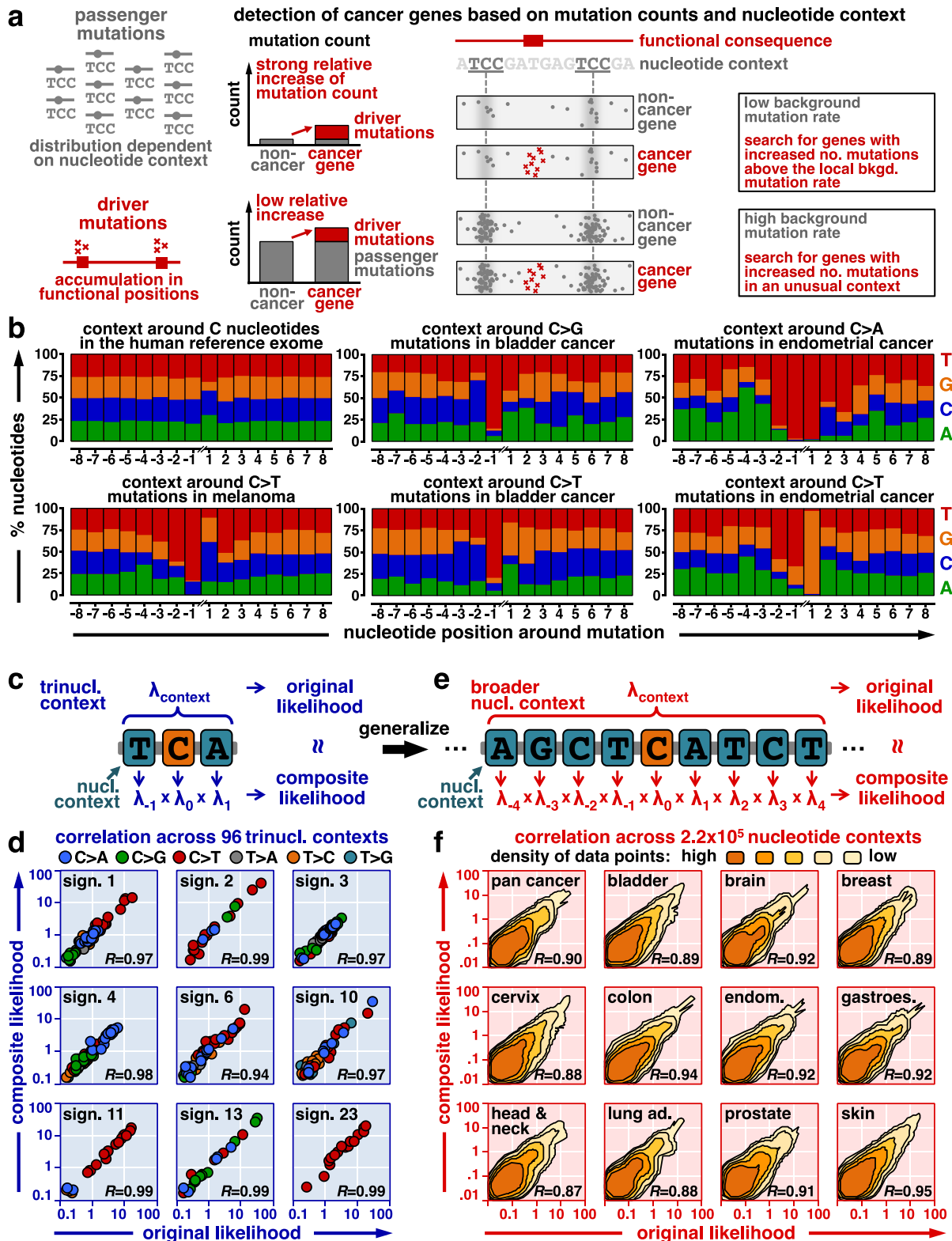
255 41. Reich, M. *et al.* GenePattern 2.0. *Nat Genet* **38**, 500-1 (2006).

256 42. Burli, R.W. *et al.* Design, synthesis, and biological evaluation of potent and selective class IIa
257 histone deacetylase (HDAC) inhibitors as a potential therapy for Huntington's disease. *J*
258 *Med Chem* **56**, 9934-54 (2013).

259 43. Maolanon, A.R., Madsen, A.S. & Olsen, C.A. Innovative Strategies for Selective Inhibition of
260 Histone Deacetylases. *Cell Chem Biol* **23**, 759-768 (2016).

261

262

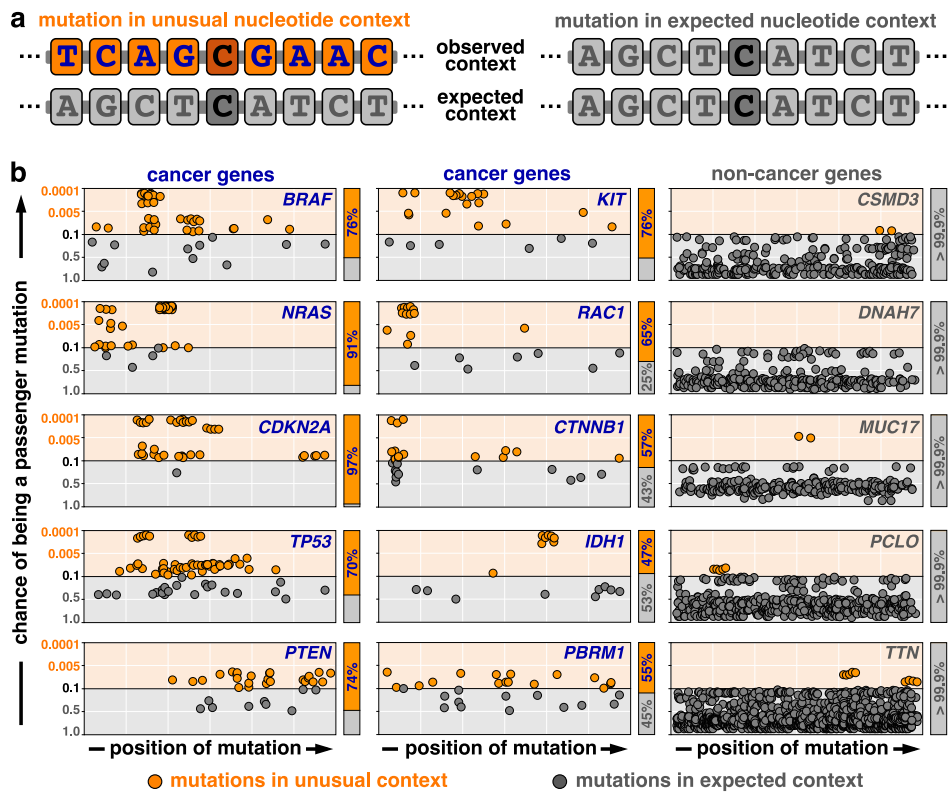


264 **Fig. 1 | A biologically informed statistical framework to discover candidate cancer genes.** **a**,
265 Schematic of our statistical framework to discover candidate cancer genes based on nucleotide
266 context. Passenger mutations accumulate in characteristic nucleotide contexts (gray, left),
267 whereas driver mutations typically accumulate in functionally relevant positions (red, left). We
268 searched for genes harboring an increased number of nonsynonymous mutations above the local
269 background mutation rate (mutational recurrence, middle). Further, we searched for genes with
270 an excess of mutations in nucleotide contexts that deviate from the characteristic nucleotide
271 context around passenger mutations (mutations in unusual contexts, right). In tumors with high
272 background mutation rates, the second criterion allowed us to actively suppress mutations in the
273 test statistics that were likely to be passenger mutations based on their surrounding nucleotide
274 context (gray). **b**, The nucleotide context around passenger mutations is visualized for three
275 cancer types with high average background mutation rates. In brief, we counted how often we
276 observed which nucleotide in the context around recurrent passenger mutations (± 8 nucleotides).
277 These plots show that the flanking 5' and 3' nucleotides have the strongest impact on the local
278 mutation probability (± 1 , trinucleotide context). However, also flanking nucleotides outside of the
279 trinucleotide context have a substantial impact on the local mutation probability, suggesting that
280 the broad nucleotide context around passenger mutations contains a relevant biological signal
281 that we needed to consider in our approach. **c-f**, To integrate this signal into our statistical
282 framework, we developed a composite likelihood model that characterizes the broad context
283 around passenger mutations. **c**, Mutation probabilities of trinucleotide contexts are commonly
284 modeled by determining the mutation probability of each possible trinucleotide context
285 independently¹¹⁻¹⁴ (original likelihood, top). Instead, we integrated the effect of the flanking 5' and
286 3' nucleotides, as well as the base substitution type as independent factors into a composite
287 likelihood model (bottom). **d**, For each classical trinucleotide mutation signature¹¹⁻¹⁴, we plotted
288 the original mutational likelihood (x-axis) against the composite likelihood (y-axis). Dot colors
289 reflect the six different base substitution types, and Pearson correlations are annotated on the
290 bottom right. These analyses revealed that mutation probabilities of trinucleotide contexts could
291 be decomposed into the effects of their central and flanking 5' and 3' nucleotides, thus
292 corroborating the validity of our composite likelihood approach for trinucleotide contexts. **e**, We
293 next generalized the composite likelihood model to broader nucleotide contexts. In parallel to our
294 approach for trinucleotide contexts, we integrated the effect of each flanking nucleotide in the

295 broad context as an independent and multiplicative factor into the composite likelihood. **f**, We
296 then counted the number of mutations in each possible 7-nucleotide context (x-axis, original
297 likelihood) and compared them with the composite likelihood (y-axis). Since the number of
298 possible nucleotide contexts was too large to be visualized directly, we plotted the data point
299 density. Similar plots for the remaining trinucleotide signatures and cancer types are shown in
300 Figures S7a-c. An analysis of the contribution of flanking nucleotides outside of the trinucleotide
301 context to the local mutation probability in the composite likelihood model is shown in Figures
302 S7d and S8.

303

304



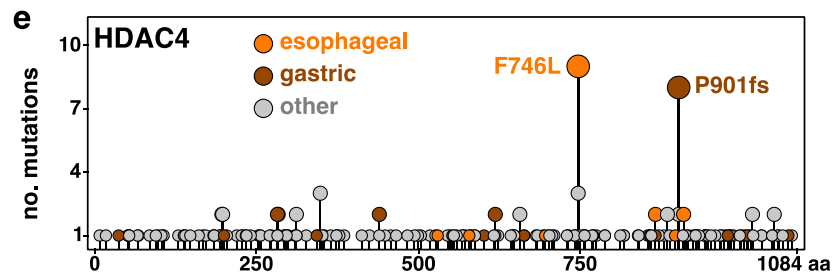
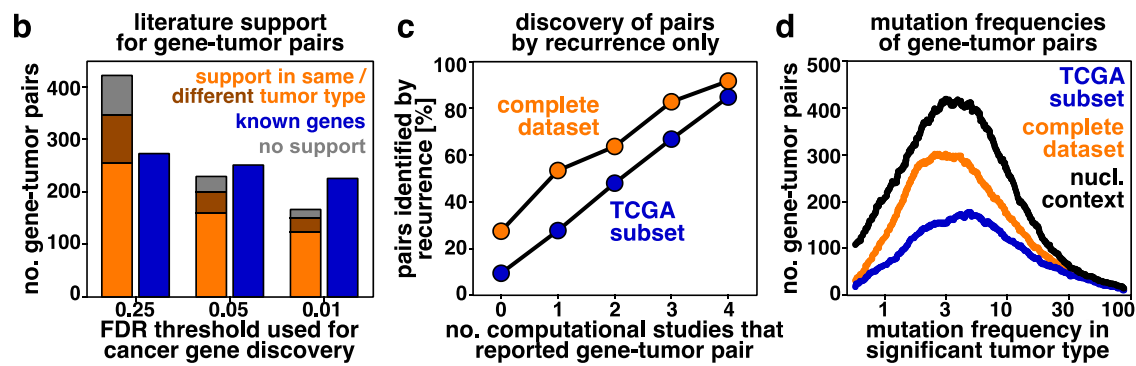
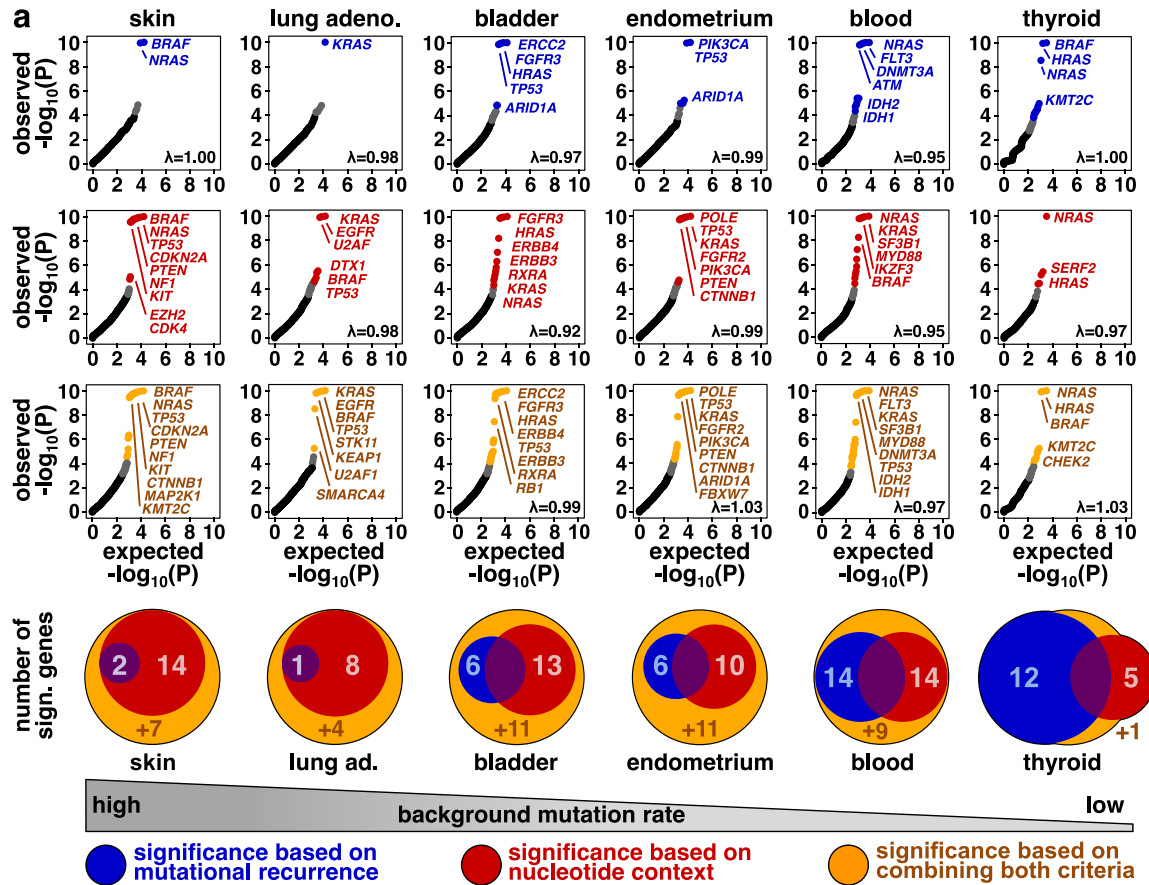
305

306 **Fig. 2 | Cancer driver genes harbor an excess of mutations in unusual nucleotide contexts.** **a**,
307 For each mutation, we compared its nucleotide context (observed context, top) with the
308 characteristic context around passenger mutations (expected context, bottom). We derived a
309 probability score that indicated whether the mutation occurred in an unusual (left, orange) or
310 expected (right, gray) nucleotide context (Methods). **b**, We corrected these probabilities for
311 multiple hypothesis testing (false-discovery rates, y-axis) and plotted them against their genomic
312 position (x-axis). In cancer genes a substantial number of mutations occurred in unusual sequence
313 contexts (left, middle). In non-cancer genes mutations in unusual sequence contexts were
314 extremely rare (right). This suggested that cancer driver genes harbor an increased number of
315 mutations in unusual nucleotide contexts that deviate from the characteristic nucleotide context
316 around passenger mutations. This observation provides a novel biological criterion to
317 discriminate between driver and passenger mutations.

318

319

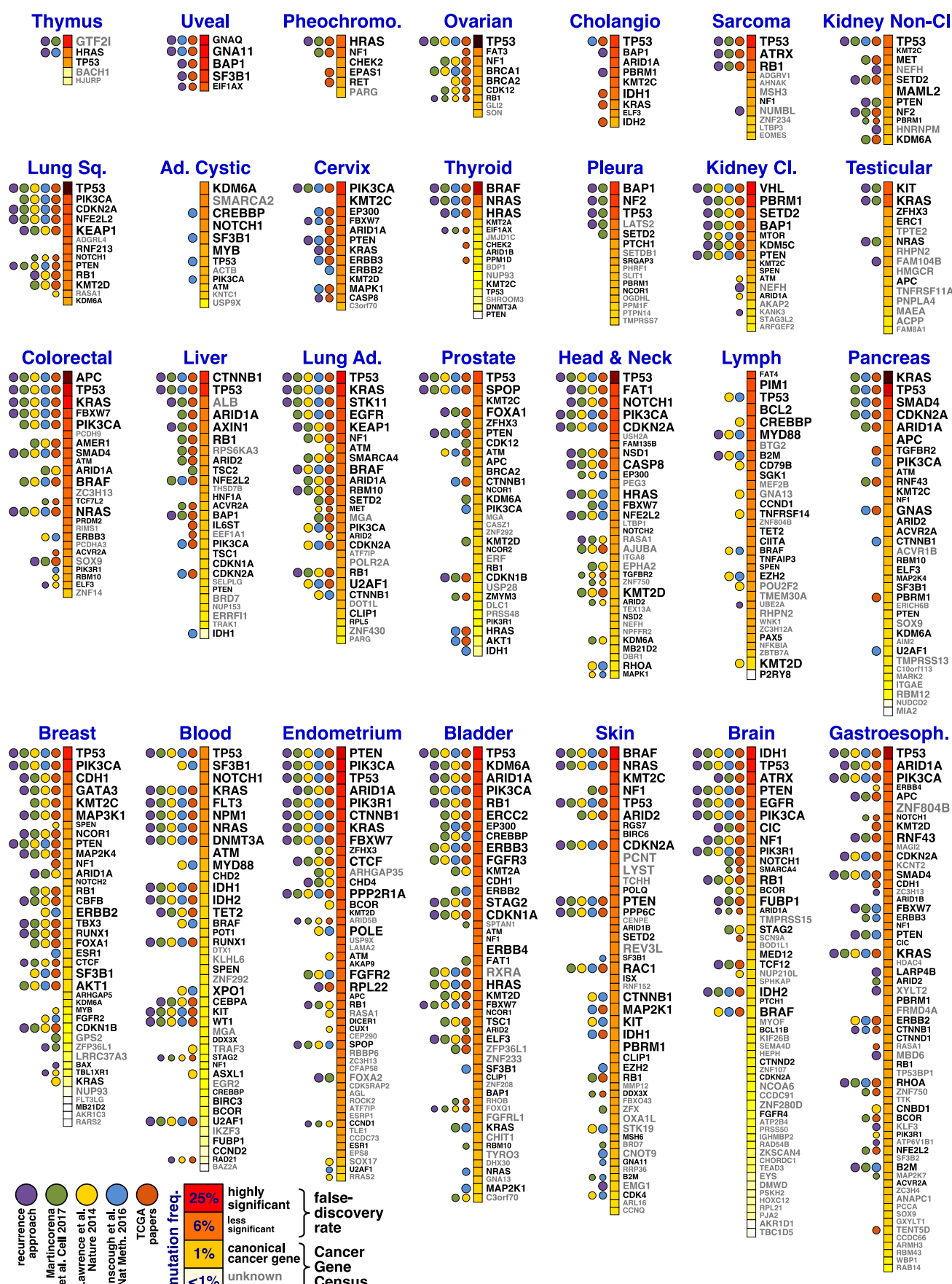
320



323 **Fig. 3 | Discovery and characterization of candidate cancer genes identified based on**
324 **nucleotide context.** **a**, We determined which genes emerged as significantly mutated (false-
325 discovery rate, FDR<0.25) based on their mutational recurrence (blue) and based on their excess
326 of mutations in “unusual” nucleotide contexts (red). Further, we identified candidate cancer genes
327 based on a statistical model that combined mutational recurrence and nucleotide context
328 (orange). We compared the expected (x-axis) and observed (y-axis) *p*-values derived from these
329 three statistical models using Q-Q-plots. Venn diagrams visualize the overlap in significant genes
330 detected with these three models (bottom). These analyses revealed that increased mutation
331 counts and unusual nucleotide contexts provide two complementary criteria for the discovery of
332 cancer genes. Integrating both aspects into a combined significance model enabled discovery of
333 candidate cancer genes across tumor types with high and low background mutation rates (left to
334 right). **b**, We stratified our findings based on their support in the literature. Known gene-tumor
335 pairs, which had been reported as significantly mutated previously, are colored in blue. Novel
336 gene-tumor pairs, which had not been reported as significantly mutated previously, are colored in
337 orange (experimental support in the same tumor type), brown (literature support in a different
338 tumor type), or gray (no support). For rigorous FDR thresholds (FDR<0.01), a majority of the
339 significant gene-tumor pairs (82%, 323/395) involved canonical cancer genes in the Cancer Gene
340 Census^{34,35}. Further, most gene-tumor pairs had been known previously or had experimental
341 literature support in the same tumor type (89%, 351/395 for FDR<0.01). For less stringent FDR
342 thresholds, the absolute number of novel findings with experimental literature support increased,
343 and the number of findings without literature support (11%, 75/697) did not exceed the expected
344 false-discovery rate (FDR<0.25). **c**, We counted for each gene-tumor pair (FDR<0.25) how many
345 previous studies reported the gene-tumor pair as significantly mutated^{4,6,7,33} (x-axis). Further, we
346 examined whether the gene-tumor pair was also identified using an established recurrence-based
347 approach³ (y-axis). The concordance between these two measures potentially reflects the fact that
348 most previous pan-cancer gene discovery studies used recurrence-based approaches to identify
349 cancer genes^{4,6,7,33}. **d**, We explored the mutation frequencies of the gene-tumor pairs that emerged
350 as significantly mutated based on their recurrence in the TCGA subset (blue), in the complete
351 dataset (orange), or when additionally considering the nucleotide context around mutations
352 (black). This density plot revealed that both the addition of 4,913 samples from TCGA-
353 independent studies and considering the nucleotide context around mutations independently

354 contributed to the discovery of rare candidate cancer genes. **e**, Exemplary evidence for the
355 candidate cancer gene *HDAC4*. Left: The distribution of *HDAC4* mutations is visualized as a needle
356 plot. For each amino acid substitution the number of samples (y-axis) is plotted against its
357 position in the peptide sequence (x-axis). Dot colors reflect the tumor types, in which the amino
358 acid substitution was detected. Right: The position of the two mutational hotspots is visualized
359 using a crystal structure⁴² (PDB: 4CBY). A previous study reported a hydrogen bond and salt
360 bridge network between W762, E764, and R730, which along with F746 form a closed
361 hydrophobic patch peripheral to the catalytic center of HDAC4⁴³ (orange). Evidence for other
362 candidate cancer genes can be found in Figures S11-S13.

363



365 **Fig. 4 | A refined catalog of driver genes involved in human cancer.** We applied our statistical
366 framework to whole-exome sequencing data from 12,004 tumors. Significant gene-tumor pairs
367 (FDR<0.25) are listed in decreasing order according to their mutation frequency, which is
368 reflected by the color of the square next to the gene name (dark red to white). The font size of the
369 gene name reflects its significance (false-discovery rate), and the font color (black vs. white)
370 indicates whether the gene is a canonical cancer gene in the Cancer Gene Census^{34,35}. To determine
371 which gene-tumor pairs had been known previously, we benchmarked our results against all
372 TCGA marker papers⁷ (orange), a meta-analysis³³ of 876 publications (blue), the tumorportal
373 database⁶ (yellow), and a pan-cancer study, which adopted the dN/dS ratio for cancer gene
374 discovery⁴ (green). We further ran an established recurrence-based approach³ on our dataset
375 (purple) to determine which gene-tumor pairs were identified based on recurrence alone. A more
376 detailed overview of the driver mutation landscape of individual tumor types is provided in
377 Figures S18-S45. An interactive visualization of these results can be found online (www.cancer-
378 genes.org).

379

| FDR < 25% Genes G-T Pairs | | FDR < 10% Genes G-T Pairs | | FDR < 5% Genes G-T Pairs | | FDR < 1% Genes G-T Pairs | | |
|--------------------------------|-----|------------------------------|-----|-----------------------------|-----|-----------------------------|-----|-----|
| Total | 379 | 697 | 298 | 562 | 252 | 484 | 201 | 395 |
| Known | 127 | 274 | 123 | 262 | 121 | 253 | 114 | 227 |
| Novel | 252 | 423 | 175 | 300 | 131 | 231 | 87 | 168 |
| ● support in same type | 110 | 257 | 85 | 198 | 70 | 161 | 50 | 124 |
| ● support in different type | 69 | 91 | 44 | 55 | 31 | 40 | 21 | 28 |
| ● no support | 73 | 75 | 46 | 47 | 30 | 30 | 16 | 16 |

380

381 **Table 1 | Stratification of candidate cancer genes by literature support.** To examine the
382 biological relevance of our findings, we stratified them based on their literature support. Genes
383 and gene-tumor (G-T) pairs that had been reported as significantly mutated in at least two
384 previous computational studies were classified as known (blue, 2nd row). Novel genes and gene-
385 tumor pairs, which had not been reported as significantly mutated previously (red, 3rd row), were
386 further stratified depending on whether there was literature support (experimental or clinical) for
387 the same tumor type in which we discovered them as significantly mutated (orange, 4th row),
388 supporting literature for a different tumor type (brown, 5th row), or no supporting data (gray, 6th
389 row). Depending on their literature support level, 94% (known, 257/274), 72% (same tumor type,
390 186/257), 23% (different tumor type, 21/91), and 3% (no support, 2/75) of the gene-tumor pairs
391 (FDR<0.25) involved canonical cancer genes present in the Cancer Gene Census^{34,35}, compared
392 with a rate of 3.8% for random gene-tumor pairs. Thus, literature support levels provide a
393 measure to prioritize our findings based on their external validity.